

# Channel Estimation Assisted Improved Timing Offset Estimation

Hlaing Minn,\**Member, IEEE*, Vijay K. Bhargava,<sup>†</sup>*Fellow, IEEE*, and Khaled Ben Letaief,<sup>‡</sup>*Fellow, IEEE*

\* Electrical Engineering Dept., University of Texas at Dallas, TX 75083-0688. (hlaing.minn@utdallas.edu)

<sup>†</sup> Electrical & Computer Engineering Dept., University of British Columbia, Canada. (vijayb@ece.ubc.ca)

<sup>‡</sup> Electrical & Electronic Engineering Dept., Hong Kong University of Science & Technology (eekhaled@ee.ust.hk)

**Abstract**—This paper presents a training signal based improved timing offset estimation method in frequency selective fading channels. A coarse timing offset estimate is first obtained by maximizing a normalized correlation metric. A coarse frequency offset estimate is similarly obtained by a correlation metric. Then a sliding observation vector based maximum likelihood approach (SOV-ML) for joint timing and frequency offset estimation is applied. This SOV-ML requires the knowledge of channel impulse response (CIR). The CIR estimate is usually affected by the coarse timing and frequency offset estimates. The key requirement for SOV-ML is to obtain a CIR estimate which is not affected (or minimally affected) by the coarse timing and frequency offsets. This paper addresses how to obtain this CIR estimate and presents how this channel estimation assists in improving the timing offset estimation. A way of complexity reduction by an adaptive scheme is also presented.

## I. INTRODUCTION

Synchronization and channel estimation are among the important issues in OFDM systems. Several approaches have been proposed for timing synchronization (e.g. [1]-[3]), frequency synchronization (e.g. [4]-[5]), joint timing and frequency synchronization (e.g. [6]-[8]) and channel estimation (e.g. [9]-[11]). These separate approaches assume perfect knowledge of the other synchronization parameters. Since errors from one task can affect the others, the idea of combined timing synchronization, frequency synchronization and channel estimation is much desirable. The combined approach not only would reflect the actual performance in the presence of non-ideal conditions but also can improve the performance by utilizing the information from one task in others.

In [12], we present a combined approach for estimation of timing offset, frequency offset, and channel for an OFDM system using a training signal. It consists of a coarse stage and a fine stage. At the fine stage, a joint timing and frequency offsets estimation is pursued by a maximum likelihood approach based on a sliding observation vector (SOV-ML). This SOV-ML approach requires the knowledge of the channel impulse response (CIR) which is not affected by timing and frequency offsets. In the presence of timing and frequency offsets, a typical channel estimation will usually give an estimate affected by those offsets and hence, it will not be applicable in the SOV-ML. In this paper, we present a channel estimation method which removes the effects of timing and frequency offsets from the CIR estimate and which is applicable in the SOV-ML. We present how this channel estimation assists in

improving the synchronization performance, in particular, timing offset estimation performance. By utilizing the knowledge of received SNR reflected in the coarse timing metric, an adaptive complexity reduction scheme is also presented.

## II. SIGNAL MODEL

The complex baseband samples of an OFDM symbol, at the sampling rate  $1/T$  ( $N$  times subcarrier spacing), are given by

$$s(k) = \frac{1}{\sqrt{N}} \sum_{n=0}^{N-1} c_n \exp(j2\pi kn/N), \quad -N_g \leq k \leq N-1 \quad (1)$$

where  $c_n$  is modulated data (zeros for null sub-carriers),  $N$  is the number of IFFT points,  $N_g$  is the number of cyclic prefix (CP) samples and  $j = \sqrt{-1}$ . Consider a frequency selective fading channel characterized by the sample-spaced channel impulse response

$$h(k) = \exp(j\phi) \sum_l h_l p(kT - \tau_l - t_0), \quad k = 0, 1, \dots, K-1 \quad (2)$$

where  $p(t)$  is the combined response of transmit and receive filters,  $t_0$  is a delay to make the filter response causal,  $\{h_l\}$  are complex path gains of the channel,  $\{\tau_l\}$  are the path delays,  $\phi$  is an arbitrary carrier phase and  $K$  is the effective maximum channel delay spread in samples. Assuming perfect sampling clock and no oscillator phase noise, the received sample can be given by

$$r(k) = \exp(j2\pi kv/N) \sum_{l=0}^{K-1} h(l)s(k-l) + n(k) \quad (3)$$

where  $v$  is the carrier frequency offset normalized by the subcarrier spacing,  $\{n(k)\}$  are independent and identically distributed, zero-mean complex Gaussian noise samples with variance  $\sigma_n^2$ ,  $-N_g + K - 1 \leq k \leq N - 1$  and  $N_g > K$ .

Define the following for a training symbol with  $N_g$  samples of CP part and  $(\beta + 1)$  samples of the useful part:

$$\begin{aligned} \mathbf{r}_\gamma(\varepsilon) &\triangleq [r(\varepsilon - \gamma) \ r(\varepsilon - \gamma + 1) \ \dots \ r(\varepsilon + \beta)]^T \\ \mathbf{h} &\triangleq [h(0) \ h(1) \ \dots \ h(K-1)]^T \\ \mathbf{W}_\gamma(v, \varepsilon) &\triangleq \text{diag}\{e^{j2\pi(\varepsilon-\gamma)v/N}, e^{j2\pi(\varepsilon-\gamma+1)v/N}, \dots, e^{j2\pi(\varepsilon+\beta)v/N}\} \\ \mathbf{n}_\gamma(\varepsilon) &\triangleq [n(\varepsilon - \gamma) \ n(\varepsilon - \gamma + 1) \ \dots \ n(\varepsilon + \beta)]^T \\ \mathbf{s}(m) &\triangleq [s(m) \ s(m-1) \ \dots \ s(m-K+1)]^T \\ \mathbf{S}_\gamma(\varepsilon) &\triangleq [s(\varepsilon - \gamma) \ s(\varepsilon - \gamma + 1) \ \dots \ s(\varepsilon + \beta)]^T \end{aligned} \quad (4)$$

where  $0 \leq \gamma \leq N_g - K + 1$  and  $-N_g + \gamma + K - 1 \leq \varepsilon \leq 0$ . If the training symbol is designed to have the same length as a

data symbol, then  $\beta + 1 = N$ . The  $(\gamma + \beta + 1 = N')$  length received samples vector,  $\mathbf{r}_\gamma(\varepsilon)$ , can be given by

$$\mathbf{r}_\gamma(\varepsilon) = e^{j2\pi\varepsilon v/N} \mathbf{W}_\gamma(v) \cdot \mathbf{S}_\gamma(\varepsilon) \cdot \mathbf{h} + \mathbf{n}_\gamma(\varepsilon) \quad (5)$$

where  $\mathbf{W}_\gamma(v) \triangleq \mathbf{W}_\gamma(v, 0)$ . In the following, the subscript  $\gamma$  will be omitted for simplicity and  $\mathbf{S}(0)$  will be denoted by  $\mathbf{S}$ .

### III. CHANNEL ESTIMATION ASSISTED IMPROVED SYNCHRONIZATION

#### A. ML Approach with A Sliding Observation Vector

Assume that an OFDM training symbol  $\{s(k) : -N_g \leq k \leq \beta\}$  is used for timing synchronization, frequency synchronization and channel estimation. The SOV-ML estimates of the timing point and the normalized carrier frequency offset, denoted by  $\varepsilon$  and  $\hat{v}$  respectively, are given by [12]

$$(\varepsilon, \hat{v})_{ML} = \underset{\tilde{\varepsilon}, \tilde{v}}{\operatorname{argmin}} \mathcal{V}(\mathbf{r}(\tilde{\varepsilon}); \hat{\mathbf{h}}, \tilde{\varepsilon}, \tilde{v}) \quad (6)$$

where

$$\mathcal{V}(\mathbf{r}(\tilde{\varepsilon}); \hat{\mathbf{h}}, \tilde{\varepsilon}, \tilde{v}) = \mathbf{r}^H(\tilde{\varepsilon})\mathbf{r}(\tilde{\varepsilon}) - 2 \cdot \Re[\mathbf{r}^H(\tilde{\varepsilon})\mathbf{W}(\tilde{v})\mathbf{S}\hat{\mathbf{h}}] + \hat{\mathbf{h}}^H \mathbf{S}^H \mathbf{S} \hat{\mathbf{h}}. \quad (7)$$

The tilde notation denotes a trial value. Detailed discussion on SOV-ML and conventional ML approaches is given in [12]. Depending on the given set of parameters, the corresponding metrics to be minimized are given by

$$\mathcal{V}_{|\hat{\mathbf{h}}, \tilde{\varepsilon}}(\mathbf{r}(\tilde{\varepsilon}); \tilde{v}) \triangleq -2 \cdot \Re[\mathbf{r}^H(\tilde{\varepsilon})\mathbf{W}(\tilde{v})\mathbf{S}\hat{\mathbf{h}}] \quad (8)$$

$$\mathcal{V}_{|\tilde{\varepsilon}}(\mathbf{r}(\tilde{\varepsilon}); \hat{\mathbf{h}}, \tilde{v}) \triangleq \mathcal{V}_{|\hat{\mathbf{h}}, \tilde{\varepsilon}}(\mathbf{r}(\tilde{\varepsilon}); \tilde{v}) + \hat{\mathbf{h}}^H \mathbf{S}^H \mathbf{S} \hat{\mathbf{h}} \quad (9)$$

$$\mathcal{V}_{|\hat{\mathbf{h}}(\mathbf{r}(\tilde{\varepsilon}); \tilde{\varepsilon}, \tilde{v}) \triangleq \mathbf{r}^H(\tilde{\varepsilon})\mathbf{r}(\tilde{\varepsilon}) + \mathcal{V}_{|\hat{\mathbf{h}}, \tilde{\varepsilon}}(\mathbf{r}(\tilde{\varepsilon}); \tilde{v}) \quad (10)$$

$$\mathcal{V}(\mathbf{r}(\tilde{\varepsilon}); \hat{\mathbf{h}}, \tilde{\varepsilon}, \tilde{v}) = \mathcal{V}_{|\hat{\mathbf{h}}(\mathbf{r}(\tilde{\varepsilon}); \tilde{\varepsilon}, \tilde{v}) + \hat{\mathbf{h}}^H \mathbf{S}^H \mathbf{S} \hat{\mathbf{h}}. \quad (11)$$

#### B. Coarse Timing and Frequency Offset Estimation

We consider a training signal with  $P + 1$  identical parts and  $M$  samples in each part. The coarse timing estimation is based on maximizing the following metric [12]:

$$\mathcal{C}(\mathbf{r}(k), M) \triangleq \frac{N' \left| \sum_{i=-\gamma}^{\beta-M} r^*(k+i) \cdot r(k+d+i) \right|}{(N' - M) \mathbf{r}^H(k) \cdot \mathbf{r}(k)}. \quad (12)$$

Due to the repetitive training structure, the metric  $\mathcal{C}(\mathbf{r}(k), M)$  would give a plateau if  $0 \leq \gamma < N_g - K + 1$  is used. Hence, we use  $\gamma = N_g$  in (12) to avoid the metric plateau.

In addition to the noise effect, the coarse timing point, in a multipath channel environment, may be at some delay with respect to the actual point due to dispersion and can cause ISI in the synchronization tasks to be performed afterwards. To prevent this, the coarse timing point can be advanced by some amount  $\lambda_c (> 0)$ . This fact is illustrated in Fig. 1(a) and (b) which show the probability mass function of the coarse timing point obtained by simulation at SNR = 10 dB. With the CP length  $N_g = 16$  and the effective maximum channel delay spread  $K = 8$ , the ISI-free range of the timing point,  $-N_g + K - 1 \leq \varepsilon \leq 0$ , is  $-9 \leq \varepsilon \leq 0$ . Fig. 1(a) shows that with a substantial amount of probability, the coarse timing point (without timing advancement) will not fall in the ISI-free region. The mean of the timing point is at some delay with respect to the actual point due to the multipath channel dispersion. With an appropriate timing advancement, the coarse timing point will most of the time fall in the ISI-free

region as can be seen in Fig. 1(b). The appropriate value of  $\lambda_c$  depends on the channel statistics such as power delay profile and effective maximum channel delay spread, the CP length and the coarse timing estimation performance. A good design rule is that for a particular channel and timing estimation method, the CP length should be such that with the timing advancement the timing point falls within the ISI-free region most of the time. If the CP length is large enough that the timing distribution fits well in the ISI-free region, then  $\lambda_c$  can be set to about half of the ISI-free length.

After obtaining the coarse timing point  $\varepsilon_c$ , coarse frequency offset estimation is performed by [12]

$$\hat{v}_c = \frac{N}{2\pi M} \operatorname{arg}\left\{ \sum_{k=0}^{M-1} u(k) \right\} \quad (13)$$

where

$$u(k) \triangleq \sum_{p=0}^{P-2} r^*(k+p \cdot M) \cdot r(k+p \cdot M + M) \quad (14)$$

and the estimation range is  $-\frac{N}{2M} < \hat{v}_c \leq \frac{N}{2M}$ .

#### C. Fine Timing and Frequency Offset Estimation

The ML estimates  $(\varepsilon, \hat{v})_{|(\varepsilon_c, \hat{v}_c)}$  which is based on the coarse estimates  $(\varepsilon_c, \hat{v}_c)$  can be obtained from (6) as

$$(\varepsilon, \hat{v})_{|(\varepsilon_c, \hat{v}_c)} = \underset{(\tilde{\varepsilon}, \tilde{v})}{\operatorname{argmin}} \{ \mathcal{V}(\mathbf{r}(\tilde{\varepsilon}); \hat{\mathbf{h}}, \tilde{\varepsilon}, \tilde{v}) : \varepsilon_c - T_1 \leq \tilde{\varepsilon} \leq \varepsilon_c + T_2, \hat{v}_c - F_1 \leq \tilde{v} \leq \hat{v}_c + F_2 \}. \quad (15)$$

Equation (15) can be implemented by first finding  $\tilde{v}$  that minimizes the metric for each  $\tilde{\varepsilon}$ , denoted by  $\hat{v}_{|\tilde{\varepsilon}}$ , and then choosing the pair  $(\tilde{\varepsilon}, \hat{v}_{|\tilde{\varepsilon}})$  that has minimum metric, denoted by  $\mathcal{V}_{|(\hat{\mathbf{h}}, \tilde{v}_c)}$ . By using (8), an ML estimate of  $v$  for a trial timing point  $\tilde{\varepsilon}$  is obtained as

$$\hat{v}_{|\tilde{\varepsilon}} = \underset{\tilde{v}}{\operatorname{argmin}} \{ \mathcal{V}_{|\hat{\mathbf{h}}, \tilde{\varepsilon}}(\mathbf{r}(\tilde{\varepsilon}); \tilde{v}) : \hat{v}_c - F_1 \leq \tilde{v} \leq \hat{v}_c + F_2 \} \quad (16)$$

with the corresponding minimum metric  $\mathcal{V}_{|(\hat{\mathbf{h}}, \tilde{\varepsilon})}(\mathbf{r}(\tilde{\varepsilon}); \hat{v}_{|\tilde{\varepsilon}})$ . Then, by using (10), an ML timing estimate is obtained as

$$\varepsilon_f = \underset{\tilde{\varepsilon}}{\operatorname{argmin}} \{ \mathcal{V}_{|\hat{\mathbf{h}}}(\mathbf{r}(\tilde{\varepsilon}); \tilde{\varepsilon}, \hat{v}_{|\tilde{\varepsilon}}) : \varepsilon_c - T_1 \leq \tilde{\varepsilon} \leq \varepsilon_c + T_2 \} \quad (17)$$

and the fine estimates are given by  $(\varepsilon_f, \hat{v}_f)$  with  $\hat{v}_f = \hat{v}_{|\varepsilon_f}$ .

#### D. Channel Estimation for Fine Synchronization

The estimation of the CIR required for ML realization of (15) is pursued in the following. At the correct sync parameters  $\varepsilon = 0$  and  $v$ , the ML estimator of  $\mathbf{h}$  is given by

$$\hat{\mathbf{h}}_{ML} = (\mathbf{S}^H \mathbf{S})^{-1} \mathbf{S}^H \mathbf{W}^H(v) \mathbf{r}(0). \quad (18)$$

Since  $v$  and  $\mathbf{r}(0)$  are unknown, one possible approach for a realizable ML estimator of (15) is to estimate  $\mathbf{h}$  by (18) with  $\mathbf{r}(0)$  and  $v$  replaced by a received vector  $\mathbf{r}(\varepsilon)$  and a frequency estimate  $\hat{v}$ , respectively, which are obtained in the coarse synchronization stage. In this case, in order to avoid the inclusion of non-training samples in the observed received vector  $\mathbf{r}_\gamma(\varepsilon)$ ,  $\gamma = 0$  would be used. Then,

$$\begin{aligned} \hat{\mathbf{h}} &= (\mathbf{S}_0^H \mathbf{S}_0)^{-1} \mathbf{S}_0^H \mathbf{W}_0^H(\hat{v}) \mathbf{r}_0(\varepsilon) \\ &= (\mathbf{S}_0^H \mathbf{S}_0)^{-1} \mathbf{S}_0^H \mathbf{W}_0^H(\hat{v}) e^{j2\pi\varepsilon v} \mathbf{W}_0(v) \mathbf{S}_0(\varepsilon) \mathbf{h} + \mathbf{n}_h \end{aligned} \quad (19)$$

where  $\mathbf{n}_h = (\mathbf{S}_0^H \mathbf{S}_0)^{-1} \mathbf{S}_0^H \mathbf{W}_0^H(\hat{v}) \mathbf{n}_0$ . Equation (19) reveals that even if  $\hat{v} = v$ , the mean of  $\hat{\mathbf{h}}$  turns out to be

$$E[\hat{\mathbf{h}}] = e^{j2\pi\varepsilon\hat{v}/N} (\mathbf{S}_0^H \mathbf{S}_0)^{-1} \mathbf{S}_0^H \mathbf{S}_0(\varepsilon) \mathbf{h} \quad (20)$$

which is not unbiased unless  $\varepsilon = 0$ . To circumvent this, we propose the following channel estimation which will be described in a general framework while the channel estimation with a repetitive training structure will be described in the next subsection. First, define the following

$$\bar{\mathbf{s}}(k) \triangleq [s(k) \ s(k-1) \ \dots \ s(k-M+1)]^T \quad (21)$$

$$\mathbf{S}(k) \triangleq [\bar{\mathbf{s}}(k) \ \bar{\mathbf{s}}(k+1) \ \dots \ \bar{\mathbf{s}}(k+N-1)]^T \quad (22)$$

$$\mathbf{g} \triangleq [\mathbf{h}^T, \mathbf{0}_{1 \times K_1}]^T \quad (23)$$

where  $\mathbf{0}_{1 \times K_1}$  is an all zero row vector of length  $K_1$ . We can observe that  $\mathbf{S}_0(\varepsilon)\mathbf{h} = \mathbf{S}(\varepsilon)\mathbf{g}$ . Then  $\mathbf{r}_0(\varepsilon)$  can be expressed as

$$\mathbf{r}_0(\varepsilon) = e^{j2\pi\varepsilon v/N} \mathbf{W}_0(v) \cdot \mathbf{S}(\varepsilon) \cdot \mathbf{g} + \mathbf{n}_0(\varepsilon). \quad (24)$$

From the definitions of (22) and (23), the following equality is observed, for  $-K_1 \leq \varepsilon \leq 0$ ,

$$\mathbf{S}(\varepsilon)\mathbf{g} = \mathbf{S}(0) \mathcal{I}(\varepsilon) \mathbf{g} \quad (25)$$

where  $\mathcal{I}(\varepsilon)$  is a  $(K+K_1) \times (K+K_1)$  unitary matrix whose elements are given by  $[\mathcal{I}(\varepsilon)]_{i,j} = [\mathbf{I}]_{(i+\varepsilon) \bmod N, j}$  with  $\mathbf{I}$  being an  $(K+K_1) \times (K+K_1)$  identity matrix. In the following,  $\mathbf{S}(0)$  will be denoted by  $\mathbf{S}$ . It is noted that  $\mathcal{I}(\varepsilon)\mathbf{g}$  is just a cyclically shifted version of  $\mathbf{g}$ . Substituting (25) into  $\mathbf{r}_0$  and applying the ML principle, at the correct sync parameters ( $\varepsilon = 0, \hat{v} = v$ ), result in

$$\hat{\mathbf{g}}(0, v) = (\mathbf{S}^H \mathbf{S})^{-1} \mathbf{S}^H \mathbf{W}_0^H(v) \mathbf{r}_0(0). \quad (26)$$

Applying (26) for  $\mathbf{r}_0(\varepsilon_c)$  with  $v$  replaced by  $\hat{v}_c$  gives

$$\hat{\mathbf{g}}(\varepsilon_c, \hat{v}_c) = (\mathbf{S}^H \mathbf{S})^{-1} \mathbf{S}^H \mathbf{W}_0^H(\hat{v}_c) \mathbf{r}_0(\varepsilon_c). \quad (27)$$

The mean of the above estimator, if  $\hat{v}_c = v$ , is

$$E[\hat{\mathbf{g}}(\varepsilon_c, \hat{v}_c)] = e^{j2\pi\varepsilon_c \hat{v}_c/N} \mathcal{I}(\varepsilon_c) \mathbf{g}. \quad (28)$$

From the above equation, we can observe that  $\mathbf{g}$  can be estimated if  $\varepsilon_c$  and  $\hat{v}_c$  are known. Since we have  $\hat{v}_c$  from the coarse synchronization stage, using an estimate  $\hat{\varepsilon}_c$  for  $\varepsilon_c$  results in an estimate of  $\mathbf{g}$  based on the pair  $(\varepsilon_c, \hat{v}_c)$  as follows:

$$\hat{\mathbf{g}}_{|(\varepsilon_c, \hat{v}_c)} = e^{-j2\pi\hat{\varepsilon}_c \hat{v}_c/N} \mathcal{I}^H(\hat{\varepsilon}_c) \hat{\mathbf{g}}(\varepsilon_c, \hat{v}_c). \quad (29)$$

Let  $\{\hat{g}(i) : i = 0, 1, \dots, K+K_1-1\}$  and  $\{\hat{g}_c(i) : i = 0, 1, \dots, K+K_1-1\}$  denote the elements of  $\hat{\mathbf{g}}_{|(\varepsilon_c, \hat{v}_c)}$  and  $\hat{\mathbf{g}}(\varepsilon_c, \hat{v}_c)$ , respectively. Then, from (23), we obtain a channel response estimate based on the pair  $(\varepsilon_c, \hat{v}_c)$  as

$$\hat{\mathbf{h}}(\varepsilon_c, \hat{v}_c) = [\hat{g}(0), \hat{g}(1), \dots, \hat{g}(K-1)]^T. \quad (30)$$

The estimate  $\hat{\varepsilon}_c$  required in (29) can be obtained as

$$\hat{\varepsilon}_c = \underset{l}{\operatorname{argmax}} \{E_h(l, \varepsilon_c) : l = 0, -1, \dots, -K_1\} \quad (31)$$

where

$$E_h(l, \varepsilon_c) = \begin{cases} \sum_{k=0}^{K-1} |\hat{g}_c((-l+k) \bmod (K+K_1))|^2, & \text{if } |\hat{g}_c(-l)| > \eta \cdot \max_i \{|\hat{g}_c(i)|\} \\ 0, & \text{otherwise.} \end{cases} \quad (32)$$

The threshold parameter  $\eta$  for selecting the first tap of the CIR is given by [8]

$$\eta_2 = \sqrt{\frac{\text{SNR}_1}{\text{SNR}_2}} \cdot \eta_1 \quad (33)$$

where  $\eta_1$  is a known value obtained from the simulation at  $\text{SNR}_1$  and  $\eta_2$  is the threshold value for  $\text{SNR}_2$ .

The above channel estimation is valid for  $-K_1 \leq \varepsilon \leq 0$  since (25) is only valid for this range. From (22), the valid

maximum value for  $K_1$  is  $M-K+1$ , or the allowable (coarse) timing offset is  $-M+K-1 \leq \varepsilon \leq 0$ , provided that  $(\mathbf{S}^H \mathbf{S})$  is invertible. Strictly speaking, this allowable timing offset range can be extended to  $-M+K-1-a \leq \varepsilon \leq 0$  by using a received vector of accordingly reduced length  $\beta+1-a$  and the  $(\beta+1-a) \times (M+1+a)$  matrix  $\mathbf{S}$ , provided that  $(\mathbf{S}^H \mathbf{S})$  is invertible. For a training symbol with multiple identical parts, the above extension is not possible and the allowable timing offset range for the channel estimation is just  $-M+K \leq \varepsilon \leq 0$ . However, in the following, this range will be extended by using the repetitive training structure.

### E. Channel Estimation with a Repetitive Training Symbol Structure for Fine Synchronization

Our training symbol has  $(P+1)$  identical parts with  $M$  samples in each part. Now, with  $K_1 = M-K$  and the repetitive parts in mind, we have

$$\mathbf{S}(\varepsilon) = \mathcal{S} \mathcal{I}(\varepsilon) \quad (34)$$

and hence (27) and (28) still hold exactly for  $-M+K-1 \leq \varepsilon \leq 0$  and approximately for  $-M+K-1-K_2 \leq \varepsilon \leq -M+K-2$  and  $1 \leq \varepsilon \leq K_3$ , for small  $K_2, K_3 > 0$ . The proximity is due to the inclusion of non-training samples in the vector  $\mathbf{r}_0(\varepsilon)$ . Note that in (25), the equality (34) does not hold.

Let  $-M+K-1-K_2 \triangleq -K_4$ . Since (27) produces a cyclically shifted version of a length  $M$  vector  $\hat{\mathbf{g}}$ , the allowable timing offset for the channel estimation is limited to  $-K_4 \leq \varepsilon \leq K_3$  where  $K_3+K_4+1 = M$ . Equation (31) now becomes

$$\hat{\varepsilon}_c = \begin{cases} l_{max} & \text{if } l_{max} \geq -K_4 \\ M+l_{max} & \text{otherwise} \end{cases} \quad (35)$$

where

$$l_{max} \triangleq \underset{l}{\operatorname{argmax}} \{E_h(l, \varepsilon_c) : l = 0, -1, \dots, -M+1\} \quad (36)$$

and together with (29), (30), (16) and (17), ML estimation (15) can now be realized for  $-K_4 \leq \varepsilon_c \leq K_3$ .

If  $\varepsilon_c < -K_4$ , the required channel estimate  $\hat{\mathbf{h}}_{req}(\varepsilon_c, \hat{v}_c)$  for the realization of (15) is given by (30) and (29) with  $\hat{\varepsilon}_c$  replaced by  $l_{max}$ . However, due to the ambiguity,  $\hat{\varepsilon}_c$  will be  $M+l_{max}$  and consequently the estimated channel response would be  $\hat{\mathbf{h}}(\varepsilon_c, \hat{v}_c) = \hat{\mathbf{h}}_{req}(\varepsilon_c, \hat{v}_c) e^{-j2\pi M \hat{v}_c/N}$  under no noise condition. Then, (15) would quite likely give a timing point around  $-M$  due to the extra factor  $e^{-j2\pi M \hat{v}_c/N}$  contained in the channel estimate. Similarly, if  $\varepsilon > K_3$ , (15) would quite likely give a timing point around  $M$ .

To solve this ambiguity, we consider three candidates, namely  $\{\varepsilon_i : i = -1, 0, 1\}$  with  $\varepsilon_i = \varepsilon_c + i \cdot M$ . If  $\varepsilon_c < -K_4$ , although  $\hat{\mathbf{h}}(\varepsilon_0, \hat{v}_c)$  would not be the proper estimate required for (15),  $\hat{\mathbf{h}}(\varepsilon_1, \hat{v}_c)$  would be the proper one since  $\varepsilon_1$  is within the allowable range. Similarly, if  $\varepsilon_c > K_3$ ,  $\hat{\mathbf{h}}(\varepsilon_{-1}, \hat{v}_c)$  would be the proper one. For each set  $(\varepsilon_i, \hat{v}_c)$ , realizing (15) results in a candidate set of fine estimates  $(\varepsilon_f, \hat{v}_f)_i$  together with the corresponding minimum metric  $\mathcal{V}_{(\varepsilon_i, \hat{v}_c)}$ . The fine estimates are then obtained as

$$(\varepsilon_f, \hat{v}_f) = \underset{(\varepsilon_f, \hat{v}_f)_i}{\operatorname{argmin}} \{\mathcal{V}_{(\varepsilon_i, \hat{v}_c)} : i = -1, 0, 1\}. \quad (37)$$

Since each candidate  $\varepsilon_i$  can produce a proper channel estimate if it is within the allowable range, the search window of  $\tilde{\varepsilon}$  can be set such that  $T_1 = K_3$  and  $T_2 = K_4$ . The allowable

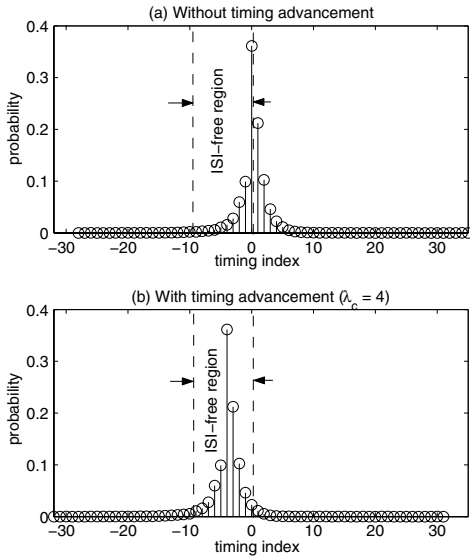


Fig. 1. The illustration of the advantage of timing advancement

coarse timing offset range is now extended to  $-M - K_4 \leq \varepsilon \leq M + K_3$  which is usually more than sufficient for the SNR of interest. This ambiguity resolution approach can appropriately be applied to the case of non-repetitive training symbol. The final timing offset may be advanced by a small amount  $\lambda_f (> 0)$  to avoid possible interference caused by occasional occurrence of positive timing offsets.

#### IV. SIMULATION RESULTS AND DISCUSSION

OFDM system parameters are  $N = 64$ , 52 used sub-carriers,  $N_g = 16$ , and QPSK modulation. The training symbol is composed of  $P + 1 = 5$  identical parts and each part is generated by 16 point IFFT of length-16 Golay complementary sequence. The channel path gains  $\{h_l; l = 0, 1, \dots, 7\}$  are WSSUS complex Gaussian with sample-spaced path delays and  $K = 8$ ,  $t_0 = 0$ . The channel power delay profile is with a -3 dB per tap decaying factor. Other parameters are  $\lambda_c = 4$ ,  $\lambda_f = 2$ ,  $v = 1.6$ ,  $F_1 = 0.1$ ,  $J_1 = 10$ ,  $J_2 = 5$ ,  $\xi = 2$ ,  $T_1 = K_3 = 4$ ,  $T_2 = K_4 = 11$ ,  $K' = K = 8$  and  $\mathcal{K} = 8$  unless stated otherwise. One packet is composed of one training symbol and 5 data symbols and the results are obtained from  $10^5$  simulation runs.

Fig. 2 (a) presents the timing offset variances of the coarse and the fine synchronization stage. Note that the coarse stage timing estimation performance represents a bench-mark for the existing correlation-based timing estimation methods (e.g. [7]) [8]. The estimation performance is much improved in the fine synchronization stage. Fig. 2 (a) also includes the timing offset variance of the fine synchronization stage with known CIR. The variance for SNR of 15 dB and above are not present for no timing offset is observed in the simulation. For the timing offsets within the ISI-free part, the system performance may not be affected. Hence, one may consider another performance measure which is more oriented to the system performance rather than the estimation performance. In

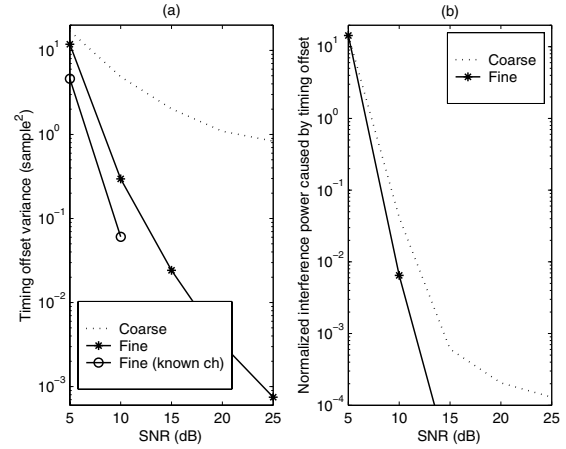


Fig. 2. Improvement of channel estimation assisted fine timing synchronization over the coarse timing synchronization

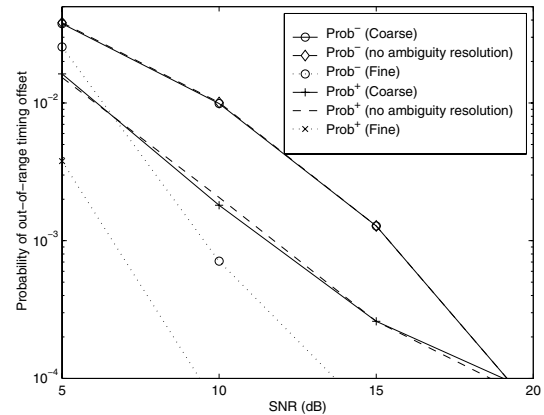


Fig. 3. Performance of timing offset ambiguity resolution for the channel estimation

this light, The average normalized interference power caused by the timing estimation (calculated as in [8]) is presented in Fig. 2 (b). Similar to the variance performance, the fine synchronization stages have less interference power than the coarse stage.

In Fig. 3, the performance of the timing offset ambiguity resolution at the fine synchronization stage is presented. Since the ambiguity-free timing offset range is  $-K_4 \leq \varepsilon \leq K_3$ , we evaluate the probability of out-of-range (i.e., out of the ambiguity-free range) timing offset in terms of the probability of timing offset less than  $-K_4$  and the probability of timing offset greater than  $K_3$ , denoted by “Prob<sup>-</sup>” and “Prob<sup>+</sup>”, respectively. These probabilities for the coarse timing and the fine timing without ambiguity resolution are essentially the same since no timing offset ambiguity is resolved. With the ambiguity resolution, the fine timing stage has well reduced these probabilities and improved the performance.

As a means of complexity reduction, adaptive ambiguity resolution approach is also evaluated. From Fig. 5(a), it can be seen that the coarse timing metric gives an indication of the received signal’s SNR. From Fig. 3, it can be observed

that the occurrence of the out-of-range timing offsets is very small for SNR values of 10 dB and higher. Hence, the mean of the coarse timing metric at SNR = 10 dB is used as a threshold for the adaptive ambiguity resolution scheme. If the coarse timing metric is higher than this threshold, no ambiguity resolution is carried out. Fig. 4(a) shows the BER performance of the proposed method with (nonadaptive) ambiguity resolution and with adaptive ambiguity resolution. Almost the same BER performance is observed. Fig. 4(b) shows the complexity gain of the adaptive ambiguity resolution approach over non-adaptive ambiguity resolution approach defined by the ambiguity resolution complexity ratio of the nonadaptive to adaptive approach. Considerable complexity gain is observed particularly at higher SNR values.

The sensitivity of the fine synchronization to the threshold value  $\eta$  is also investigated. In Fig. 5(b), the variances of the fine timing offset estimation with different threshold values ( $\eta^*$ ,  $\eta^*/2$  and  $3\eta^*/2$ ) are presented. The value used for  $\eta^*$  at 10 dB SNR is  $\eta_{10}^* = 0.2$  [8] and the  $\eta^*$  values at other SNR are calculated from (33). The figure also indicates that the fine timing offset variance is not so sensitive to the threshold values within the range from  $\eta^*/2$  to  $3\eta^*/2$ .

## V. CONCLUSIONS

This paper discusses channel estimation assisted improved synchronization. With the aids of the coarse timing and frequency offset estimates, the fine synchronization stage is performed by a maximum likelihood approach with a sliding observation vector (SOV-ML). The corresponding likelihood function requires a channel impulse response (CIR) estimate which is not affected by the timing and frequency offsets. The proposed channel estimation removes the effects of coarse timing and frequency offsets from the CIR estimate and facilitates the implementation of the SOV-ML improved synchronization. The proposed channel-estimation-assisted timing estimation achieves a substantial performance improvement. A coarse-timing-metric-assisted adaptive scheme for complexity reduction is also presented which achieves essentially the same BER performance.

## ACKNOWLEDGMENT

This work was supported in part by the School of Engineering and Computer Science at the University of Texas at Dallas and in part by the Natural Sciences and Engineering Research Council (NSERC) of Canada.

## REFERENCES

- [1] M. Speth, F. Classen and H. Meyr, "Frame synchronization of OFDM systems in frequency selective fading channels," *Proc. Vehicular Tech. Conf.*, Phoenix, Arizona, USA, May 1997, pp. 1807-1811.
- [2] D. Landström, S. K. Wilson, J.J. van de Beek, P. Ödling and P. O. Börjesson, "Symbol time offset estimation in coherent OFDM systems," *IEEE Trans. Commun.*, Vol. 50, Issue 4, pp. 545-549, Apr. 2002.
- [3] B. Yang, K. Ben Letaief, R. S. Cheng and Z. Cao, "Timing recovery for OFDM transmission," *IEEE J. Select. Areas in Commun.*, Vol. 18, No. 11, pp. 2278-2290, Nov. 2000.
- [4] P.H. Moose, "A technique for orthogonal frequency division multiplexing frequency offset correction," *IEEE Trans. on Commun.*, Vol. 42, No. 10, pp. 2908-2914, Oct 1994.

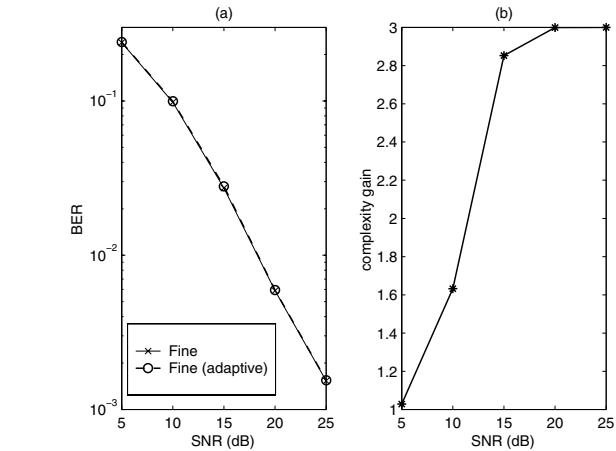


Fig. 4. BER performance and complexity gain of the adaptive ambiguity resolution scheme

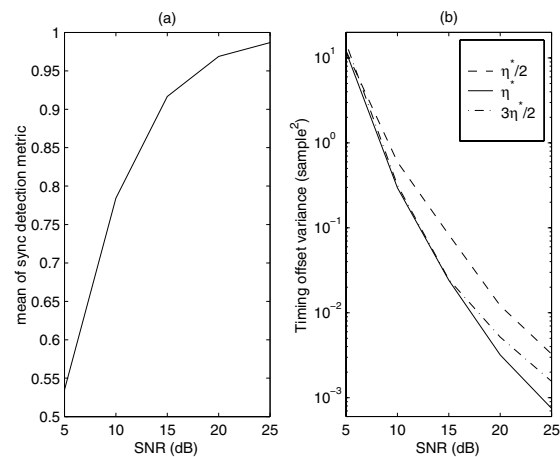


Fig. 5. (a) Mean of the sync detection metric  $C^2(\mathbf{r}(\varepsilon_c), N_g)$ . (b) Performance with different threshold values for the first channel tap selection

- [5] M. Morelli and U. Mengali, "An improved frequency offset estimator for OFDM applications," *IEEE Commun. Letters*, Vol. 3, No. 3, Mar 1999, pp. 75-77.
- [6] J.-J. van de Beek, M. Sandell and P.O. Börjesson, "ML estimation of time and frequency offset in OFDM systems" *IEEE Trans. Signal Proc.*, Vol. 45, no. 7, July 1997, pp. 1800-1805.
- [7] T. M. Schmidl and D. C. Cox, "Robust frequency and timing synchronization for OFDM," *IEEE Trans. Commun.*, Vol. 45, No. 12, Dec 1997, pp. 1613-1621.
- [8] H. Minn, V. K. Bhargava and K. Ben Letaief, "A robust timing and frequency synchronization for OFDM systems," *IEEE Trans. Wireless Commun.*, Vol. 2, No. 4, pp. 822-839, July 2003.
- [9] O. Edfors, M. Sandell, J.-J. van de Beek, S. K. Wilson and P. O. Börjesson, "OFDM channel estimation by singular value decomposition," *IEEE Trans. Commun.* vol. 46, pp. 931-939, Jul 1998.
- [10] Y. Li, L. J. Cimini, Jr., and N. R. Sollenberger, "Robust channel estimation for OFDM systems with rapid dispersive fading channels," *IEEE Trans. Commun.*, vol. 46, pp.902-915, Jul 1998.
- [11] B. Yang, K. Ben Letaief, R. S. Cheng and Z. Cao, "Channel estimation for OFDM transmission in multipath fading channels based on parametric channel modeling," *IEEE Trans. Commun.*, vol. 49, No. 3, pp. 467-479, Mar 2001.
- [12] H. Minn, V. K. Bhargava and K. Ben Letaief, "A combined timing and frequency synchronization and channel estimation for OFDM," *accepted in IEEE ICC 2004, Communications Theory Symposium*.